NUMERICAL SIMULATION OF THE MOTION OF DROPS ON AN INCLINED SURFACE[*]

M. M. TAFRESHI AND S. MORTAZAVI[**]

Dept. of Mechanical Engineering, Isfahan University of Technology, 84156-83111, Isfahan, I. R. of Iran
Email: saeedm@cc.iut.ac.ir

Abstract– The flow of two-dimensional drops suspended in an inclined channel is studied by numerical simulations at non-zero Reynolds numbers. The flow is driven by the acceleration due to gravity, and there is no pressure gradient in the flow direction. The equilibrium position of a drop is studied as a function of the Reynolds number, the Capillary number, the inclination angle and the density ratio. It is found that the drop always lags the undisturbed flow. More deformable drops reach a steady state equilibrium position that is farther away from the channel floor. For drops that are heavier than the ambient fluid, the equilibrium position moves away from the channel floor as the Reynolds number is raised. The same trend is observed when the inclination angle with respect to horizontal direction increases. The behavior agrees with computational modeling of chute flow of granular materials. A drop that is lighter than the ambient fluid reaches a steady state equilibrium position closer to the channel floor when the Reynolds number or inclination angle increases. Simulations of 40 drops in a relatively large channel, show that drops move away from the channel floor when the density ratio is larger than unity.

Keywords– Reynolds number, capillary number, density ratio, inclination angle, bond number, equilibrium position

1. INTRODUCTION

The migration of neutrally buoyant solid particles and drops was studied by Goldsmith & Mason [1, 2] in tube flow at a nearly zero Reynolds number.

Hiller & Kowalewski [3] conducted experiments on a very dilute suspension of droplets in a plane Poiseuille flow in the creeping flow limit. They found that drops with low viscosity ratio (0.1) eventually concentrate at the channel axis. At a high viscosity ratio (1), however, the concentration peak moved to a position between the wall and the centerline. The effect of inertia on the motion of particles in Poiseuille flow was studied experimentally by Segre & Silberberg [4, 5]. They performed experiments with a dilute suspension of neutrally buoyant solid particles for a wide range of Reynolds numbers and particle sizes. They observed that solid particles migrate away from both the tube axis and the wall, forming a concentrated layer at about half the distance between the tube axis and the wall. This effect was further investigated by Karnis, Goldsmith & Mason [6-8] using spherical particles and drops. They found that deformable drops migrate to the tube axis if their viscosity is low (similar to the creeping flow limit), but behave like solid particles at high viscosity ratios, and settle at a distance halfway between the channel wall and the centerline.

Ho & Leal [9] obtained the equilibrium position, and the trajectory of a small, neutrally buoyant sphere in a linear shear flow, as well as in Poiseuille flow, using a regular perturbation expansion for small particle Reynolds numbers. Their results were in good agreement with experimental observations of

Segre & Silberberg [4, 5]. Additional analytical studies have been reported by Vasseur & Cox [10], and Cox & Hsu [11]. They found that the equilibrium position was slightly closer to the wall than that predicted by Ho & Leal. Particles close to the wall also had a different migration velocity.

Recently, the migration of deformable drops in shear flows was studied by numerical simulations at zero Reynolds number using boundary-integral method. The two-dimensional simulation of a few droplets performed by Zhou & Pozrikidis [12, 13] for Couette flow, and by Zhou & Pozrikidis [14] for Poiseuille flow, showed that deformable drops migrate away from the walls.

Feng, Hu & Joseph [15, 16] conducted two-dimensional simulations of solid particles in a Poiseuille flow at finite Reynolds numbers using a finite element method. Their results were in good agreement with the perturbation theory of Ho & Leal (1974)[9], and the experiments of Segre & Silberberg [4, 5].

Recently, Mortazavi and Tryggvason [17] studied the motion of a single drop at non-zero Reynolds numbers in Poissuille flow. The migration of the drop was studied as a function of the Reynolds number, the Weber number and the viscosity ratio.

Campbell and Brennen [18] performed a computer simulation for chute flow of granular materials. Their results consisted of the velocity distribution, density and granular temperature. They considered the effect of density and shear rate on the granular temperature.

Griggs et al [19] studied the creeping motion of deformable drops on an inclined surface in three dimensions.

Bayareh and Mortazavi [20] performed a dynamic simulation of deformable drops in simple shear flow at finite Reynolds numbers. The flow was studied as a function of the Reynolds number and the Capillary number, and a shear thinning behavior was observed.

Nourbakhsh and Mortazavi [21] studied the motion of deformable drops in Poiseuille flow at non-zero Reynolds numbers. The density distribution of drops across the channel was studied as a function the Reynolds number and the Capillary number. Also, the effective viscosity increased with the Reynolds number. Goodarzi and Mortazavi [22] studied the lateral migration of a buoyant drop in simple shear flow at finite Reynolds numbers.

Here, we study the motion of two-dimensional drops suspended on an inclined surface at non-zero Reynolds numbers. The lateral migration of a drop is examined as a function of the non-dimensional parameters of the flow. The study is similar to that performed by Griggs et al [19] at zero Reynolds number. The flow is driven by the component of the acceleration due to gravity in the flow direction. The component of the gravitational acceleration normal to flow direction is also included.

2. GOVERNING EQUATIONS AND NUMERICAL METHOD

a) Governing equations

The flow of suspension of drops in another fluid at non-zero Reynolds numbers is governed by the Navier-Stokes equations. The Navier-Stokes equations are written in conservative form with variable physical properties. The surface tension is added to the formulation by a delta function that acts at the interface:

$$\frac{\partial(\rho \mathbf{u})}{\partial t} + \nabla.(\rho \mathbf{u}\mathbf{u}) = -\nabla P + \nabla.\mu(\nabla \mathbf{u} + \nabla \mathbf{u}^T) - \int (\sigma\kappa\mathbf{n})\delta(x - X(s,t))ds \qquad (1)$$

Hence, the equations are valid for both the drop and the ambient fluid. Here, $\mathbf{u}$ is the velocity field, p is the pressure, ρ is the density, μ is the viscosity, σ is the interfacial tension, κ is the curvature for two-dimensional flows, $\mathbf{n}$ is an outward unit normal to the drop surface, and δ is a two-dimensional delta function. $\mathbf{x}$ is the Eulerian coordinate system; $\mathbf{X}$ is a Lagrangian representation of the interface and s is a

parameter defined on the interface. The fluids are incompressible and immiscible with constant material properties. Therefore:

$$\nabla.\mathbf{u} = 0 \tag{2}$$

$$\frac{D\rho}{Dt} = 0 \tag{3}$$

$$\frac{D\mu}{Dt} = 0 \tag{4}$$

In our computations it is assumed that the drop viscosity is the same as the viscosity of the suspending medium. We note that Eqs. (3) and (4) state that the physical properties (density and viscosity) of a fluid element does not change as one follows it along its path.

The geometry of the flow is shown in Fig. 1.
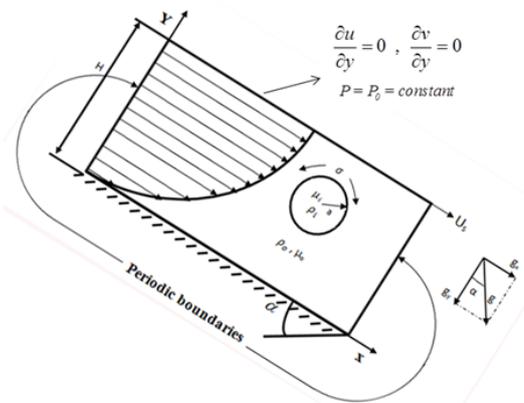
Fig. 1. Channel geometry

The computational domain is periodic in the x-direction. It is bounded by a no slip wall at the bottom, and a free surface at the top. The channel has an inclination angle with respect to horizontal direction. The flow is driven by the component of gravitational acceleration in the x-direction (g_x), and the pressure gradient in the flow direction is zero. The velocity profile in the absence of drops is a parabolic velocity profile formed by g_x.

The governing non-dimensional numbers of the flow are: the Reynolds number Re, the Capillary number Ca, the ratio of the viscosity of the drop fluid to that of the ambient fluid $\gamma = \frac{\mu_i}{\mu_o}$, the density ratio $\lambda = \frac{\rho_i}{\rho_o}$ and the inclination angle *α*. A characteristic velocity can be defined based on the acceleration due to gravity, the physical properties of the suspending fluid and the channel height: $U_c = \frac{\rho_o g H^2}{2\mu_o}$ .The Reynolds number is defined based on this characteristic velocity and the channel height (H): $Re = \frac{\rho_o^2 g H^3}{2\mu_0^2}$. The Capillary number is also defined based on this characteristic velocity: $Ca = \frac{U_c \mu_0}{\sigma} = \frac{\rho_0 g H^2}{2\sigma}$. We should note that the velocity at the free surface of the channel in the absence of drops (U_s) is related to component of the gravitational acceleration in the flow direction (g_x) by : $U_s = \frac{\rho_0 g_x H^2}{2\mu_0}$.

The Bond number is defined as: $B=\Delta\rho g a^2/\sigma$, where $\Delta\rho$ is the density difference between the drop and suspending medium, a is the radius of un-deformed drop, g is the acceleration due to gravity, and σ is the interfacial tension.

We emphasize that the present work includes inertia effects even though it is performed in two dimensions. This feature of the current effort exempts it from other works done at zero Reynolds number.

b) Numerical method

The governing equations for the flow of drops in a channel are solved by a Finite Difference/Front Tracking method developed by Unverdi & Tryggvason [23]. A second order projection method is used to solve the Navier-Stokes equations on a staggered grid. Both the convective and diffusion terms are discretized by central differencing and a second order predictor-corrector scheme is used for time marching. The interface between the two fluids is represented by marker points that are advected by the flow velocity. The surface tension is calculated by finding the curvature of this moving grid and distributing it onto the stationary grid. The interface is reconstructed at every time step, thus preventing any numerical diffusion. The elliptic equation for the pressure is solved by a fast Poisson solver (FISHPACK) when the density of drop fluid is the same as the suspending medium. It is solved by a multi-grid method (Adams) for density ratios other than unity. A detailed convergence study of a single drop motion is given by Mortazavi & Tryggvason (2000).

3. RESULTS

a) Resolution test and validation

The dependence of results to grid resolution was checked by simulating the motion of a drop in the channel with three grid resolutions. The channel is assumed to be vertical ($\alpha=90^o$). The other flow parameters are: Re =20, Ca =0.1, λ =1.0. Figure 2a presents the lateral position of the drop versus time. There is about 5 percent change in the lateral equilibrium position when the computational grid is refined from 64×64 to 256×256 grid points. The accuracy of the result was further checked by releasing a drop from different initial locations inside the channel. Figure 2b shows the lateral position versus the axial location for four drops released from different locations. All drops migrate nearly to the same equilibrium position as the flow proceeds.

(a)   (b)
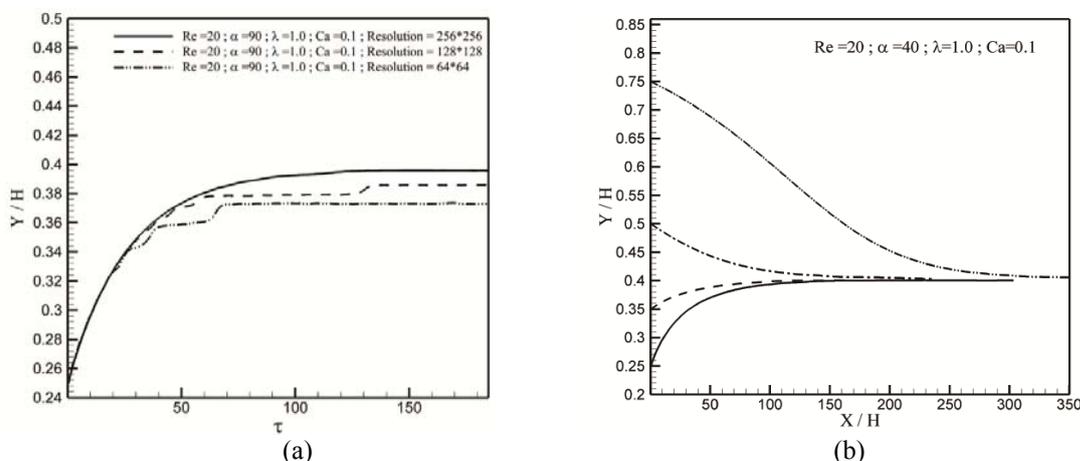
Fig. 2. Effect of grid resolution on the lateral equilibrium position of a drop

Three dimensional simulations performed by Griggs *et al.* [19] at zero Reynolds number predicts the steady state shape of drop for different Bond numbers and inclination angles. Since the present work entails two-dimensional simulations where inertia effects are also included, comparison between drop shapes at steady state is not relevant. However, qualitative agreement was observed between two efforts (not plotted).

b) Effect of deformation

The effect of deformation on the equilibrium position of drop was investigated by changing the Capillary number. Different flow conditions were examined. Drop shapes at steady state equilibrium position are plotted in Fig. 3 for two Capillary numbers.
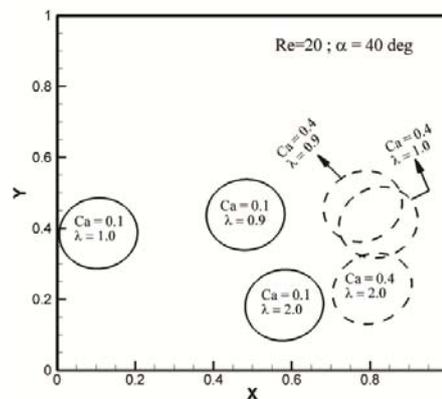
Fig 3. Steady state drop shapes at different Capillary numbers and density ratios.

Three density ratios are considered (λ=0.9,1.0,2.0). The equilibrium position of drop is plotted versus the Capillary number in Fig. 4a. The equilibrium position moves towards the free surface as the Capillary increases .We recall that the drift by the channel floor is enhanced for more deformable drops. In other words, the wall repulsion force increases as the Capillary number is raised. This has been observed by Zhou et al, and Mortazavi et al in their numerical simulations of drops suspended in shear flows. We note that the equilibrium position is closer to channel floor for heavier drops (λ=2.0) than for lighter drops (λ=0.9).

The circulation around the drop is plotted as a function of the axial location for two Capillary numbers in Fig. 4b. For neutrally buoyant drops (λ=1.0), and drops that are lighter than suspending medium, the circulation increases in magnitude as the Capillary number is reduced. For nearly circular drops (low Capillary number), the velocity gradient across the drop diameter is larger. As a result, circular drops rotate faster inside the channel. It should be pointed out that the rotation of drop in the flow also depends on the slip velocity that will be addressed later. For drops that are heavier than the ambient fluid (λ=2.0), the circulation of the drop is larger in magnitude at a higher Capillary number (Ca=0.4). This is due to large change in the slip velocity that occurs at this density ratio. The slip velocities of drops are plotted in Fig. 4c for two Capillary numbers. For density ratios less than or equal to one, the slip velocities weakly change with Capillary number, so the circulation of drop is not significantly affected by the slip velocity. For heavier drops (λ=2.0) the slip velocity changes to a large extent with Capillary number. The slip velocity is larger in magnitude at a low Capillary number (Ca=0.1). Since the slip velocity is significantly larger at lower Capillary number, the drop circulation is smaller in magnitude (Fig. 4b). The large slip velocity at this Capillary number reduces the effective velocity gradient across the drop diameter, which in turn reduces the rotation of the drop. We note that in all the simulations presented in this paper, the slip velocity is negative, so the drop always lags the flow.

(a)

(b)

(c)
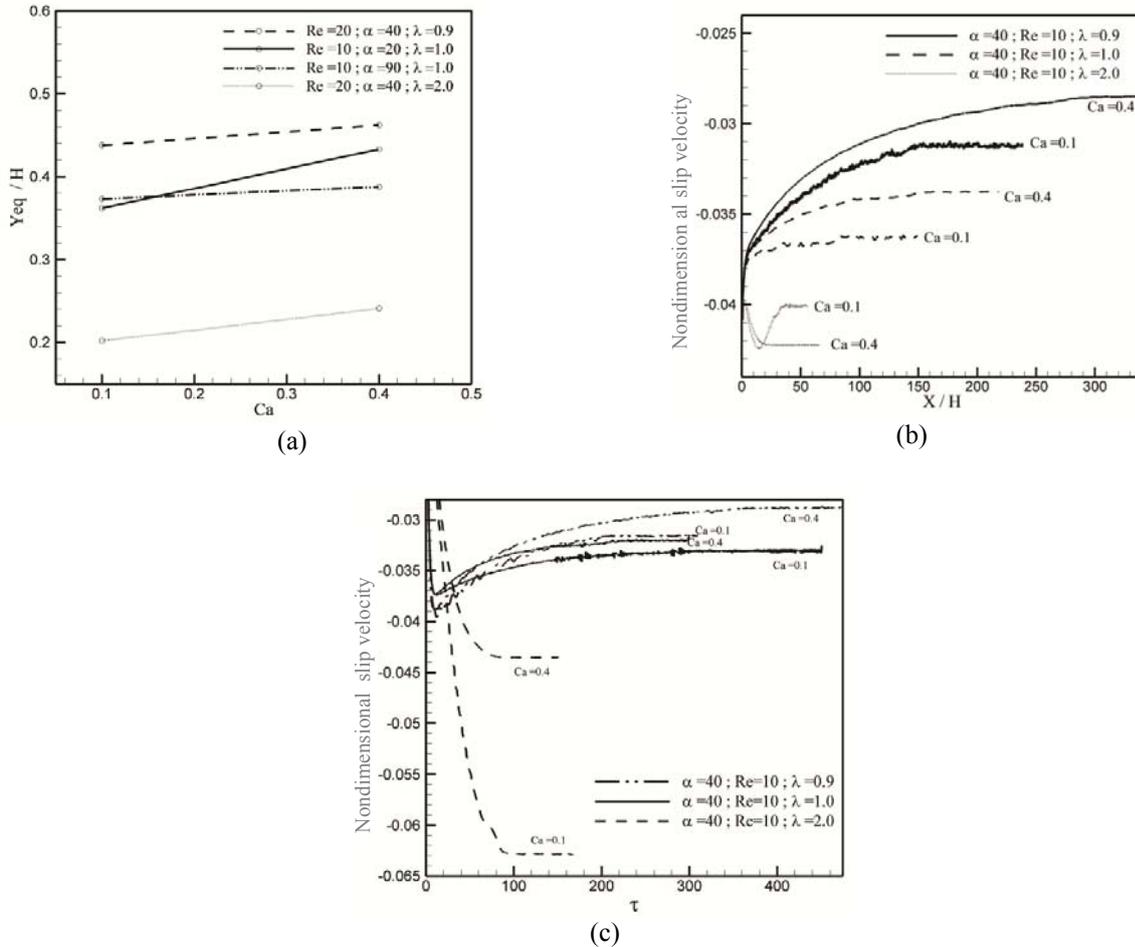
Fig 4. (a) Equilibrium position versus Capillary number, (b) Circulation versus axial location,
(c) Slip velocity versus time for different Capillary numbers

Figure 5 depicts streamlines for two Capillary numbers (Ca=0.1, Ca=0.4). The streamlines are plotted when drop has reached the steady state equilibrium position.

(a)

(b)
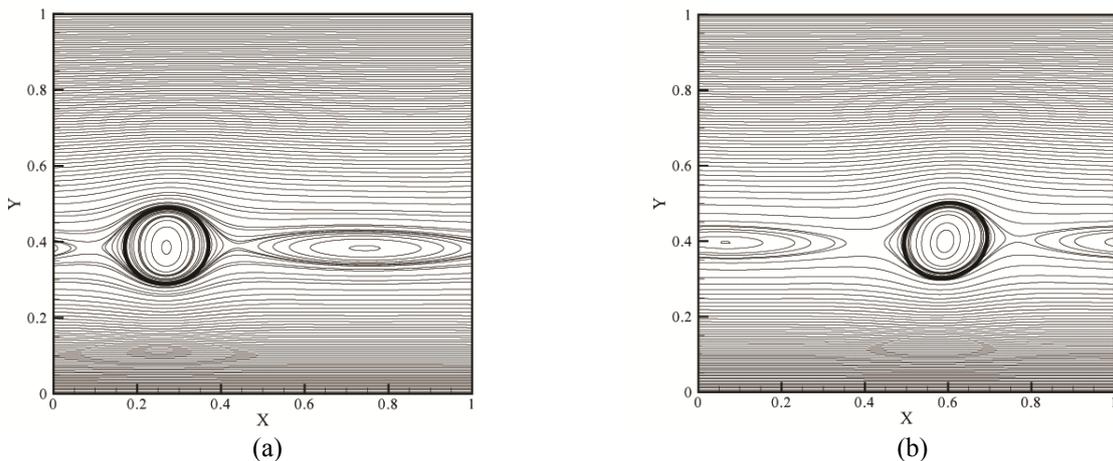
Fig 5. Streamline for a drop at steady state equilibrium position,
(a) Re=40, λ=1.0, α=40°, Ca=0.1, (b) Re=40, λ=1.0, α=40°, Ca=0.4

c) Effect of the Reynolds number

We present results that show the effect of the Reynolds number on the equilibrium position of a drop in a range of Capillary numbers and density ratios.

(a)   (b)
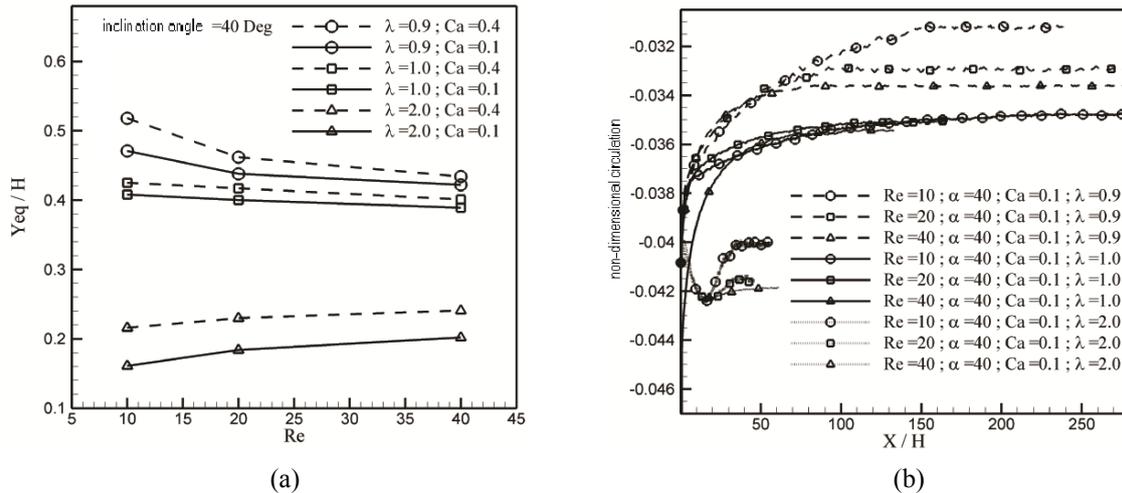
Fig. 6. (a) Equilibrium position versus the Reynolds number, (b) Circulation versus the
axial location at different Reynolds numbers and density ratios

Figure 6a shows the lateral equilibrium position as a function of the Reynolds number .Two Capillary numbers are considered (Ca=0.1 , Ca=0.4). The density ratio varies from 0.9 to 2.0. For density ratios less than or equal to one the equilibrium position moves towards the channel floor as the Reynolds number increases. For a neutrally buoyant drop (λ=1.0) the equilibrium position weakly depends on the Reynolds number.

The effect is similar to that found by Feng *et al.* for solid particles in Poiseuille flow. In other words, the equilibrium position moves slightly to the wall when the Reynolds number increases. The lateral force due to curvature of the velocity profile which points towards the wall enhances with the Reynolds number. This trend is also the same for a lighter drop (λ=0.9). However, the equilibrium position is more sensitive to the Reynolds number. For a lighter drop the buoyancy force points towards the free surface. As a result, the drift by the wall (or geometric blocking as referred by Feng *et al.*) weakens. This moves the equilibrium position closer to the channel floor. We note that the slip velocity of the drop is not significantly affected by the Reynolds number for density ratios less than or equal to one (Fig. 7). Therefore, the Magnus type lift force is nearly unaffected by the Reynolds number.

The trend reverses for heavier drops (λ=2.0).The equilibrium position moves towards the free surface with the Reynolds number. For heavier drops the buoyancy force points towards the channel floor. As a result, the lubrication force or geometric blocking enhances with the Reynolds number. This moves the equilibrium position away from the channel floor. The circulation around the drop is plotted for different Reynolds numbers in Fig. 6b. The circulation of drop increases with the Reynolds number for all density ratios. The magnitude of circulation is larger for heavier drops. This is basically due to larger velocity gradient across the drop. The equilibrium position of heavier drops is closer to the channel floor, therefore these drops are subject to a larger shear rate inside the channel. The slip velocities of drops are also plotted in Fig. 7. The slip velocities are unaffected by the Reynolds number for density ratios less than or equal to one (Figs. 7a and 7b). However, for heavier drops (λ=2.0) the magnitude of the slip velocity decreases with the Reynolds number (Fig. 7c).

This is an inertia effect that is enhanced for heavier drops. For drops that are heavier than the ambient fluid, the buoyancy force points towards the channel floor and enhances as the Reynolds number is raised. (Here, the inclination angle is constant, and when g_x increases, g_y increases as well). It should be pointed out that at this density ratio (λ=2.0) the circulation of drop increases with the Reynolds number (Fig. 6b), Also, the slip velocity decreases with the Reynolds number (Fig. 7c). So, it is anticipated that the Magnus lift force that points towards the free surface is unaffected by the Reynolds number.

M. M. Tafreshi and S. Mortazavi

(a)

(b)

(c)
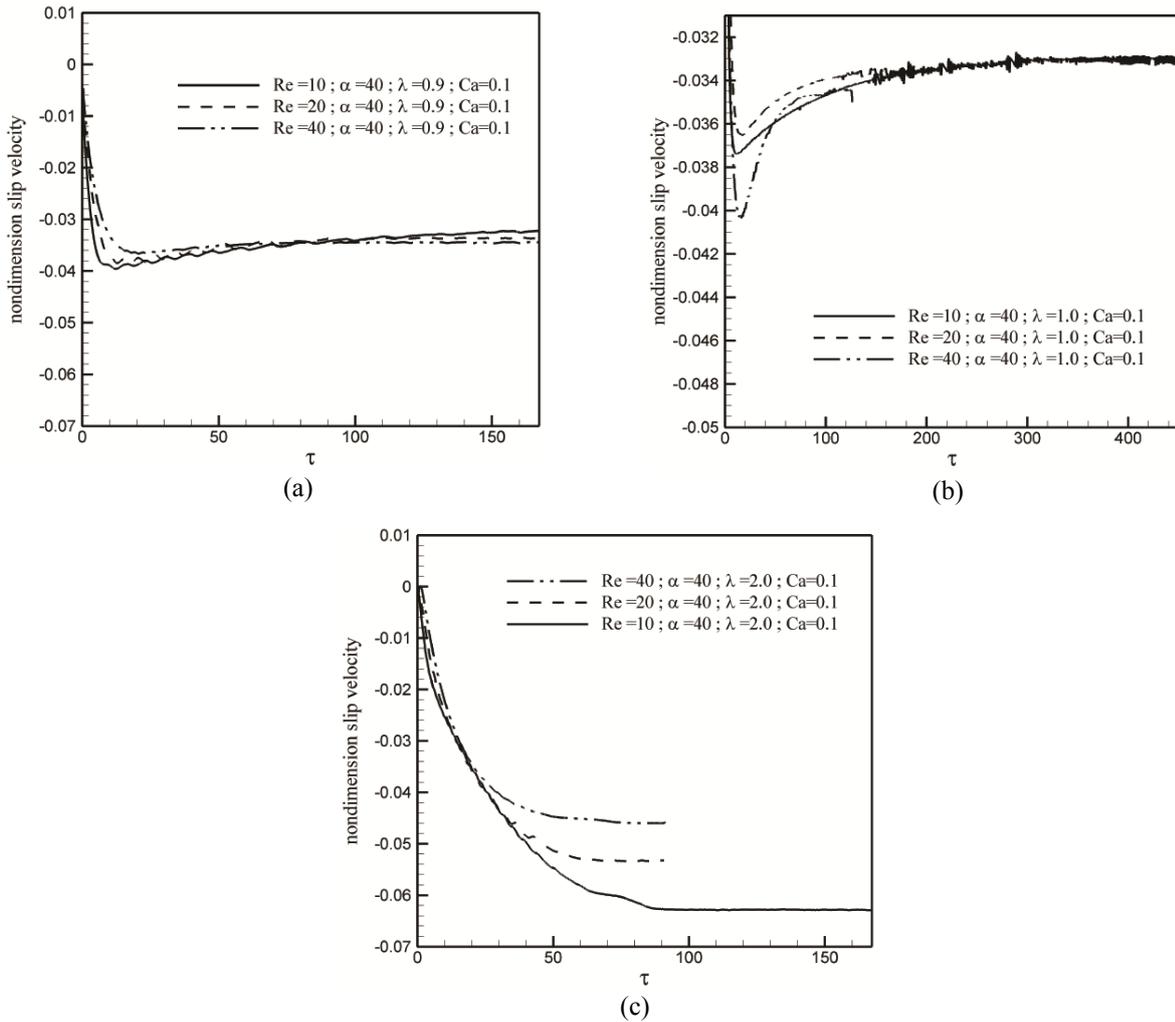
Fig 7. Slip velocity versus time for different Reynolds numbers at (a) λ=0.9, (b) λ=1.0, (c) λ=2.0

It can be seen that the equilibrium position of the drop is mainly due to the balance between the drift by the wall, and the force by the curvature of the velocity profile. This mechanism for the lateral migration of the drop persists in many drops collisions as well. This will be elaborated in more detail in section 3.6.

Figure 8 shows the drop deformation for three Reynolds numbers at a constant Capillary number (Ca=0.4). The drop deformation is nearly the same for the three Reynolds numbers considered. As a result, the proper non-dimensional number for the interfacial tension is the Capillary number.
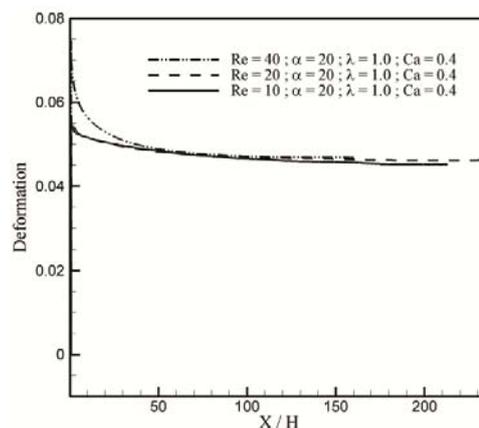
Fig. 8. Drop deformation versus axial location for different Reynolds numbers at a constant Capillary number

d) Effect of inclination angle

The effect of inclination angle was investigated by changing the channel slope with respect to horizontal direction, while the acceleration due to gravity was fixed. In other words, when the orientation angle relative to horizontal increases, the free surface velocity of channel increases. So, the Reynolds number based on the free surface velocity increases as well.
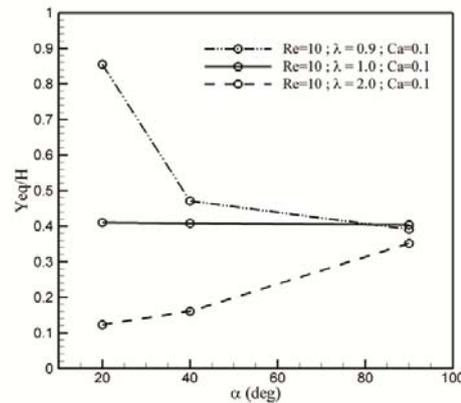
Fig. 9. Equilibrium position versus the inclination angle of channel for different density ratios

Figure 9 presents the lateral equilibrium position of drop as a function of the inclination angle. The effect is similar to that observed in section 3.3 (effect of the Reynolds number).For neutrally buoyant drops (λ=1.0) the equilibrium position weakly depends on the orientation angle. The equilibrium position moves slightly towards the channel floor as the orientation angle increases. The effect is mainly due to an increase of the Reynolds number based on the free surface velocity. For light drops (λ=0.9), the equilibrium position is strongly affected by the inclination angle. The buoyancy force, which points towards the free surface is reduced by increasing the inclination angle. As a result, the equilibrium position moves towards the channel floor. The same effect persists in case of heavy drops. The buoyancy force that is towards the channel floor decreases with the inclination angle. Also, since the Reynolds number based on the free surface velocity increases, the drift by the wall (geometric blocking) enhances as well. The overall behavior is that the equilibrium position moves away from the channel floor. We note that the trend observed here is similar to that observed in section 3.3. However, the variation of the equilibrium position with orientation angle is more enhanced compared to the effect of the Reynolds number. Here, the buoyancy force normal to the flow direction decreases with the inclination angle. And, at the same time the Reynolds number based on the free surface velocity increases. Campbell and Brennen observed a similar behavior in chute flow of granular materials. Their computational modeling showed that rigid particles moved farther away from the channel bottom as the inclination angle was increased.

e) Effect of density ratio

Figure 10 presents the lateral equilibrium position as a function of density ratio. The effect was addressed implicitly in previous sections. Three inclination angles are examined. The equilibrium position moves to the channel bottom as density ratio is raised. This is basically the effect of buoyancy force that acts on the drop. At a high inclination angle (α=90°) the effect is minimal since the component of the gravitational acceleration normal to flow direction is reduced. Figure 11 shows the average axial velocity across the channel along with the undisturbed velocity profile. The axial velocity is scaled by the maximum velocity at the free surface of the channel. Three density ratios are considered. As it was pointed out earlier, the drop always lags the flow, and the magnitude of slip velocity increases as the density ratio is increased.
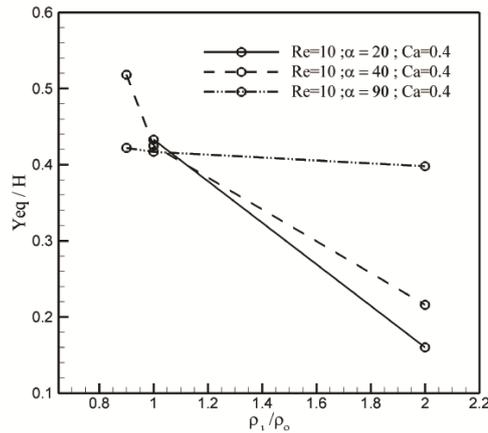
Fig 10. Equilibrium position versus density ratio for different inclination angles
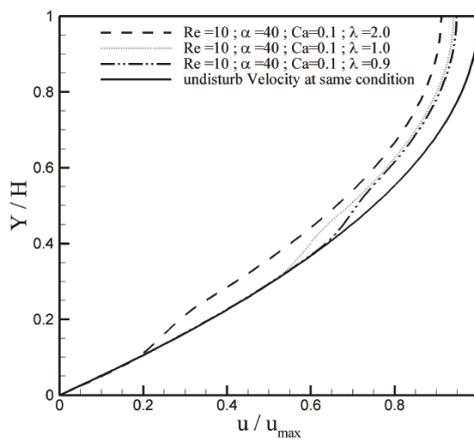
Fig 11. Average steady state velocity profile for different density ratios, λ=0.9, 1.0, 2.0

f) Simulation of 40 drops in a relatively large channel

We present dynamic simulations of 40 drops in a channel at finite Reynolds numbers. The channel height is relatively larger than its length (3 by 1).

The intention of the study is to examine the density distribution and random energy of drops across the channel. The simulations are similar to that examined by Cambpell and Brennen (1985) in granular flow regime. Here, a brief parametric study is outlined, specifically the effect of Reynolds number is studied by two simulations, and a detailed study is left for future investigations. Drops are initially placed close to the channel floor in a regular array and their relative positions are slightly perturbed.
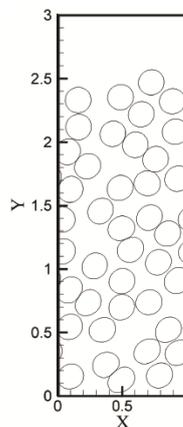
Fig 12. A snap shot of drops close to the end of simulation, Re=10, Ca=0.8, λ=2.0, α=40°

Figure 12 shows a snap shot of drops close to the end of simulation. Drops on the average, have moved about 50 times the periodic length of the channel. The flow conditions are: Re=10, Ca=0.8, λ=2.0 and α=40$^{\text{o}}$.

Figure 13a presents the density distribution of drops across the channel for two Reynolds numbers. The channel height is divided into 10 equal slices and the number of drops in each slice are counted and divided by the total number of drops. This density distribution is then averaged over time after an initial transient period. It is observed that drops move away from the channel floor, and the maximum density occurs at a position away from the floor. The discontinuity in density profile is due to the method it was calculated, i.e. the density of drops is only evaluated in each slice. Since the number of slices across the channel are limited (10), density goes through a jump when moving from one slice to another slice. The behavior is similar to that observed by Campbell and Brennen [18] in computer simulation of granular materials. As the Reynolds number increases, the peak in density distribution moves closer to the wall. The average fluctuation energy of the flow is plotted across the channel for two Reynolds numbers in Fig. 13b. As expected, the fluctuation energy increases with the Reynolds number. It has a maximum at some location close to the channel floor and decreases as one moves towards the channel free surface. This behavior is also similar to that observed by Campbell and Brennen [18].

Further investigation of behavior of drops as a function of the effective parameters of flow is left for future investigations (see Mortazavi and Tafreshi [24] for a detailed study).

(a)   (b)
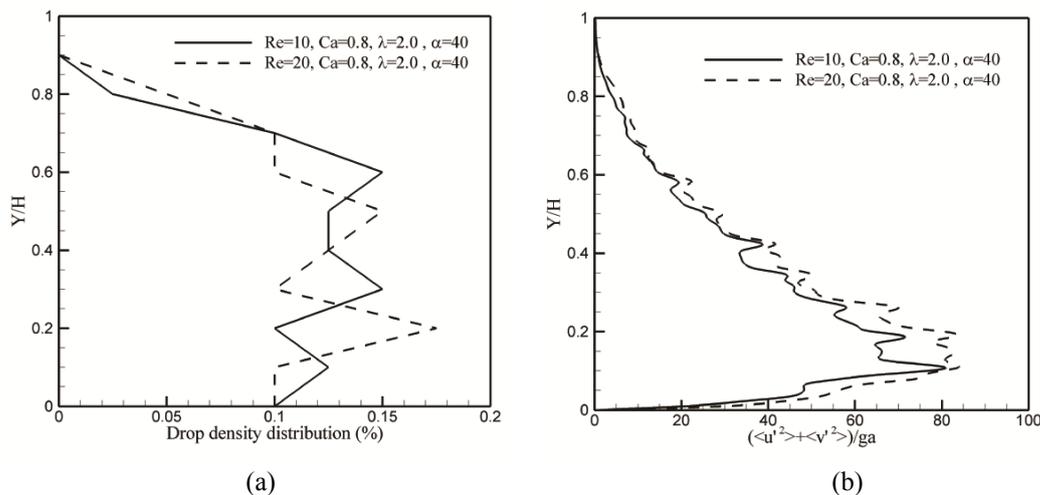
Fig. 13. Density distribution and fluctuation energy of drops across the channel for two Reynolds numbers

4. CONCLUSION

The motion of deformable drops suspended in an inclined channel was predicted using numerical simulations at non-zero Reynolds numbers. The flow was investigated as a function of the Capillary number, the Reynolds number, the inclination angle and the density ratio. The present study led us to the following conclusions:

1. The lateral equilibrium position of drop depends on drop deformation. The equilibrium position moves away from the channel floor as the Capillary number or drop deformation increases. The result is consistent with experimental findings of Karnis et al and numerical simulations of Zhou & Pozrikidis at zero Reynolds number.

2. For drops that are heavier than the ambient fluid, drops tend to stay farther away from the channel floor as the Reynolds number increases. On the contrary, neutrally buoyant drops and drops that are lighter than the surrounding medium move towards the channel floor when the Reynolds number is raised.

3. When the inclination angle of the channel with respect to horizontal direction increases, the equilibrium position of a heavier drop moves away from the channel floor. Result is in agreement with computational modeling of Campbell and Brennen on chute flow of granular materials. For neutrally buoyant drops the equilibrium position weakly changes with inclination angle. For drops that are lighter than the ambient fluid, the equilibrium position moves towards the channel floor as the inclination angle increases.

4. Drops that are suspended in an inclined channel always lag the undisturbed flow.

5. As the density ratio increases, drops move to an equilibrium position closer to channel floor.

6. Simulations of 40 drops in a channel showed that drops move away from the channel floor when the density ratio is larger than one, and the maximum concentration occurs at a distance away from channel floor. Also, the fluctuation energy of the flow gets maximum at a specific distance from the channel floor.

REFERENCES

1. Goldsmith, H. L. & Mason, S. G. (1961). Axial migration of particles in poiseuille flow. *Nature*, Vol. 190, pp. 1095-1096.

2. Goldsmith, H. L. & Mason, S. G. (1962). The flow of suspensions through tubes. I. Single spheres, rods, and discs. *Journal of Colloid Science*, Vol. 17, pp. 448-476.

3. Hiller, W. & Kowalewski, T. A. (1986). An experimental study of the lateral migration of a droplet in a creeping flow. *Experiments in Fluids*, Vol. 5, pp. 43-48.

4. [4]Segré, G. & Silberberg, A. (1962). Behaviour of macroscopic rigid spheres in Poiseuille flow Part 1. Determination of local concentration by statistical analysis of particle passages through crossed light beams. *Journal of Fluid Mechanics*, Vol. 14, pp. 115-135.

5. Segré, G. & Silberberg, A. (1962). Behaviour of macroscopic rigid spheres in Poiseuille flow Part 2. Experimental results and interpretation. *Journal of Fluid Mechanics*, Vol. 14, pp. 136-157.

6. Karnis, A., Goldsmith, H. L. & Mason, S. G. (1963). Axial migration of particles in poiseuille flow. *Nature*, Vol. 200, pp. 159-160.

7. Karnis, A., Goldsmith, H. L. & Mason, S. G. (1966). The kinetics of flowing dispersions: I. Concentrated suspensions of rigid particles. *Journal of Colloid and Interface Science*, Vol. 22, pp. 531-553.

8. Karnis, A., Goldsmith, H. L. & Mason, S. G. (1966). The flow of suspensions through tubes: V. Inertial effects. *The Canadian Journal of Chemical Engineering*, Vol. 44, pp. 181-193.

9. Ho, B. P. & Leal, L. G. (1974). Inertial migration of rigid spheres in two-dimensional unidirectional flows. *Journal of Fluid Mechanics*, Vol. 65, pp. 365-400.

10. Vasseur, P. & Cox, R. G. (1976). The lateral migration of a spherical particle in two-dimensional shear flows. *Journal of Fluid Mechanics*, Vol. 78, pp. 385-413.

11. Cox, R. G. & Hsu, S. K. (1977). The lateral migration of solid particles in a laminar flow near a plane. *International Journal of Multiphase Flow*, Vol. 3, pp. 201-222.

12. Zhou, H. & Pozrikidis, C. (1993). The flow of suspensions in channels: Single files of drops. *Physics of Fluids A: Fluid Dynamics*, Vol. 5, pp. 311-324.

13. Zhou, H. & Pozrikidis, C. (1993). The flow of ordered and random suspensions of two-dimensional drops in a channel. *Journal of Fluid Mechanics*, Vol. 255, pp. 103-127.

14. Zhou, H. & Pozrikidis, C. (1994). Pressure-driven flow of suspensions of liquid drops. *Physics of Fluids*, Vol. 6, pp. 80-94.

15. Feng, J., Hu, H. H. & Joseph, D. D. (1994). Direct simulation of initial value problems for the motion of solid bodies in a Newtonian fluid Part 1. Sedimentation. *Journal of Fluid Mechanics*, Vol. 261, pp. 95-134.

16. Feng, J., Hu, H. H. & Joseph, D. D. (1994). Direct simulation of initial value problems for the motion of solid bodies in a Newtonian fluid. Part 2. Couette and Poiseuille flows. *Journal of Fluid Mechanics*, Vol. 277, pp. 271-301.

17. Mortazavi, S. & Tryggvason, G. (2000). A numerical study of the motion of drops in Poiseuille flow. Part 1. Lateral migration of one drop. *Journal of Fluid Mechanics*, Vol. 411, pp. 325-350.

18. Campbell, C. S. & Brennen, C. E. (1985). Chute flows of granular material: Some computer simulations. *Journal of Applied Mechanics*, Vol. 52, pp. 172-178.

19. Griggs, A. J., Zinchenko, A. Z. & Davis, R. H. (2008). Gravity-driven motion of a deformable drop or bubble near an inclined plane at low Reynolds number. *International Journal of Multiphase Flow*, Vol. 34, pp. 408-418.

20. Bayareh, M. & Mortazavi, S. (2011). Three-dimensional numerical simulation of drops suspended in simple shear flow at finite Reynolds numbers. *International Journal of Multiphase Flow*, Vol. 37, pp. 1315-1330.

21. Nourbakhsh, A., Mortazavi, S. & Afshar, Y. (2011). Three-dimensional numerical simulation of drops suspended in Poiseuille flow at non-zero Reynolds numbers. *Physics of Fluids*, Vol. 23, pp. 123303-11.

22. Goodarzi, S. & Mortazavi, S. (2012). Numerical simulation of a buoyant suspending drop in plane Couette flow: the equilibrium position of the drop. *Iranian Journal of Science and Technology, Transactions of Mechanical Engineering*, Vol. 36, No. M1, pp. 69-82.

23. Unverdi, S. O. & Tryggvason, G. (1992). Computations of multi-fluid flows. *Physica*, Vol. 60, pp. 70-83.

24. Mortazavi, S. & Tafreshi, M. M. (2013). On the behavior of suspension of drops on an inclined surface. *Physica A*, Vol. 392, pp. 58-71.